AMERICAN PSYCHOLOGICAL ASSOCIATION

Journal of Experimental Psychology: General

ISSN: 0096-3445

2023, Vol. 152, No. 12, 3433–3439
https://doi.org/10.1037/xge0001441

Gravitational and Retinal Reference Frames Shape Spatial Memory

Raffaele Tucciarelli[1, 2, 3], Elisa R. Ferrè[1, 4], Elena Amoruso[1, 2], Elena Azañón[5, 6, 7], and Matthew R. Longo[1]
[1] Department of Psychological Sciences, Birkbeck, University of London
[2] Institute of Cognitive Neuroscience, University College London
[3] The Warburg Institute, University of London
[4] Department of Psychology, Royal Holloway, University of London
[5] Institute of Psychology, Otto-von-Guericke University Magdeburg
[6] Center for Behavioral Brain Sciences, Otto-von-Guericke University Magdeburg
[7] Department of Behavioral Neurology, Leibniz Institute for Neurobiology

When reproducing the remembered location of dots within a circle, judgments are biased toward the center of imaginary quadrants formed by imaginary vertical and horizontal axes. This effect may result from the heightened precision in the visual system for these orientations in a *retinotopic* reference frame, or alternately on the internal representation of gravity. We dissociated reference frames defined by the retina and by gravity by having participants locate dots from memory in a circle when their head was upright (aligned with gravity) versus tilted 30° to the left (misaligned with gravity). We mapped the structure of spatial prototypes in a data-driven way using a novel "imaging" procedure. We calculated the rotation of the prototype maps which maximized the similarity between postures, letting us quantify the contribution of each reference frame. Spatial categories are determined by a combination of reference frames, with clear contributions from both gravitational and retinal factors.

Public Significance Statement

Our ability to remember the location we saw something is shaped both by our actual memory and by categorical information about the environment in which we saw it. For example, when people remember the location of a dot they saw appear in a circle, their judgments indicate that they have implicitly divided the circle into four quadrants by imposing imaginary horizontal and vertical lines. We investigated whether these lines are determined by horizontal and vertical on the eye, or relative to gravity. Participants reproduced the remembered locations of dots in a circular frame while their head was upright or tilted to the side. The results show that both verticality on the eye and relative to gravity are used.

Keywords: spatial perception, reference frames, spatial memory, categories, gravity

Categories provide a fundamental source of structure for perception and memory (Harnad, 1987). Classic studies have shown systematic biases in spatial memory, demonstrating that fine-grained memory traces are combined with categorical spatial prototypes (Cheng et al., 2007; Huttenlocher et al., 1991). For example, when people reproduce the remembered location of a dot within a circle,

---

Matthew R. Longo https://orcid.org/0000-0002-2450-4903

Raffaele Tucciarelli, Elisa R. Ferrè, Elena Azañón, and Matthew R. Longo contributed equally to this work.

This research was supported by a grant from the European Research Council (ERC2013-StG-336050) under the FP7 to Matthew R. Longo. All data, analysis scripts, and supplementary material have been made publicly available via Open Science Framework and can be accessed at https://osf.io/9z54m/. The design and analysis plan for the experiments were not preregistered.

Raffaele Tucciarelli served as lead for data curation, formal analysis, and software. Elisa R. Ferrè contributed equally to investigation and served in a supporting role for methodology. Elena Amoruso served as lead for investigation and served in a supporting role for conceptualization and writing–review and editing. Elena Azañón contributed equally to software. Matthew R. Longo served as lead for funding acquisition, project administration, supervision, and writing–original draft and served in a supporting role for data curation and formal analysis. Raffaele Tucciarelli, Elisa R. Ferrè, Elena Azañón, and Matthew R. Longo contributed equally to conceptualization. Raffaele Tucciarelli and Matthew R. Longo contributed equally to visualization. Raffaele Tucciarelli, Elisa R. Ferrè, and Elena Azañón contributed equally to writing–review and editing. Raffaele Tucciarelli, Elena Azañón, and Matthew R. Longo contributed equally to methodology.

Correspondence concerning this article should be addressed to Matthew R. Longo, Department of Psychological Sciences, Birkbeck, University of London, Malet Street, London WC1E 7HX, United Kingdom. Email: m.longo@bbk.ac.uk

their judgments are biased toward the center of mass of each imagery quadrant of the circle divided along the vertical and horizontal meridians (Huttenlocher et al., 1991, 2004; Lipinski et al., 2010; Wedell et al., 2007). This shows that people implicitly, and automatically, segment geometric shapes, and use this imaginary structure to shape working memory for object location. Location memory is thus biased toward particular regions, which serve as *spatial prototypes*, pulling in nearby stimuli. These spatial prototypes function essentially as Bayesian priors for memory such that reconstructed locations involve a weighted combination of fine-grained memory traces and prototypical locations. Huttenlocher and colleagues have shown that despite the bias introduced by such spatial prototypes, it can nevertheless reduce overall error when memory in imprecise (Duffy et al., 2006; Huttenlocher et al., 2004; Newcombe & Huttenlocher, 2000).

We recently developed a novel procedure for "imaging" the structure of spatial prototypes of a shape in a data-driven way (Azañón et al., 2020). By analyzing the overall pattern of directional memory errors, we identified regions of shapes that tended to attract responses, and regions that tended to repel them, and therefore we could visually estimate the category boundaries imposed by the participants. We used this method on various geometrical shapes to show that spatial prototypes are defined with respect to multiple frames of reference, based both on intrinsic features of the object itself (e.g., axes of symmetry) and features extrinsic to the object (e.g., orientation relative to vertical). These extrinsic reference frames potentially include both *egocentric* reference frames based on the perceiver's own body and sensory apparatus and *allocentric* reference frames based on features of the environment. The findings of Azañón and colleagues are important as they show that people do not exclusively use extrinsic reference frames of reference, as previously argued (Engebretson & Huttenlocher, 1996; Huttenlocher et al., 2004; Wedell et al., 2007), but the imposition of vertical and horizontal axes is nuanced and depends on the context and the type of information available.

Some researchers have suggested that the division of a shape by horizontal and vertical meridians is based on the heightened precision in the visual system for these orientations in a *retinotopic* reference frame (Engebretson & Huttenlocher, 1996; Huttenlocher et al., 2004). This interpretation is consistent with a substantial body of evidence that visual sensitivity is enhanced for stimuli aligned with the vertical and horizontal meridians compared with diagonal stimuli (Campbell et al., 1966; Heeley & Timney, 1988; Orban et al., 1984), a phenomenon known as the "oblique effect" (Appelle, 1972). Neurophysiological studies of orientation-selective neurons in the monkey visual cortex have found that a disproportionate number of neurons show selectivity for vertical and horizontal stimuli (De Valois et al., 1982; Mansfield, 1974). Similarly, studies in humans have shown stronger responses for vertical and horizontal stimuli in the visual cortex using both electrophysiological evoked responses (Maffei & Campbell, 1970) and functional magnetic resonance imaging (Furmanski & Engel, 2000).

It is also possible, however, that this division is based on an absolute reference for spatial perception, such as the internal representation of the gravitational vector. On Earth, gravity is a constant downward acceleration of approximately 9.8 m/s^2. Perceiving the direction of gravity is essential for balance and orientation in space. The vestibular system signals the brain the orientation of one's own head relative to gravity. Vestibular information is integrated with signals from vision, proprioception, and somatosensory system to build a coherent representation of the right way up, the so-called *gravitational vertical* (Berthoz, 1996). The perception of the gravitational vertical is very accurate when observers are upright, but biases emerge when people are tilted away from the gravitational vector. That is, tilting either the body or the head biases verticality perception of visual lines (Van Beuzekom & Van Gisbergen, 2000). A high degree of roll tilt (>30°–60°) induces an Aubert Effect, or A-effect, wherein the verticality perception was biased toward the longitudinal body axis (Aubert, 1861). Conversely, smaller roll tilts cause a Müller Effect, or E-effect, wherein the verticality perception is biased away from the direction of tilt (Müller, 1916).

Since the gravitational vertical defines what is up and what is down and deviations thereof in a gravitational field, it might not be so surprising that this information is used as a reference for behavior. Studies in rats have shown that gravity modulates the representation of spatial layout in hippocampal place cells (Grieves et al., 2020) and grid cells (Casali et al., 2019). In nonhuman primates, gravity similarly modulates scene structure in the ventral visual pathway (Vaziri & Connor, 2016) and tuning functions of orientation-selective visual neurons (Horn & Hill, 1969; Rosenberg & Angelaki, 2014). Studies in humans have also identified broader contributions of the gravitational vector to perception and cognition, including the geometry of defensive peripersonal space (Bufacchi & Iannetti, 2016), perceived body-part weight (Ferrè et al., 2019) and location (Gallagher et al., 2021), and even aesthetic judgments (Gallagher & Ferrè, 2018).

Our previous study (Azañón et al., 2020) provided evidence for the use of multiple reference frames in determining spatial prototype effects. Here, we applied similar logic to quantify the roles of retinal and gravitational reference frames in determining the structure of spatial prototypes, which in turn reflect the observed systematic biases in spatial memory. Participants saw a dot appear inside a circle, and after a 1 s delay reproduced the remembered location of the dot in another circle that appeared at a different location on the monitor (Figure 1). By analyzing the pattern of directional memory error vectors (i.e., the deviation of remembered location compared to actual location), we quantified for each location within the circle to what extent it tended to attract versus repel remembered location, using the procedure we recently developed (Azañón et al., 2020). In separate conditions, the participant's head was aligned with the gravitational vertical (i.e., head upright) or misaligned (i.e., head tilted 30° to the left). Participants viewed the screen through a circular aperture, which prevented the use of environmental cues.

Method

Participants

Twenty individuals (10 men, 10 women) between 17 and 49 years of age (*M*: 21.7 years) participated. Eighteen were right-handed by self-report, and two left-handed. Participants were naïve regarding the purpose of the experiment, provided written informed consent, and were paid for participation. Procedures were approved by the local research ethics committee at Royal Holloway, University of London, and were in line with the principles of the Declaration of Helsinki.

In our previous study using this paradigm (Azañón et al., 2020), the key statistical test to distinguish reference frames was in Experiment 4 and gave an effect size of $d = 0.872$. A power analysis

Figure 1

Experimental Procedure and Analysis Methodology

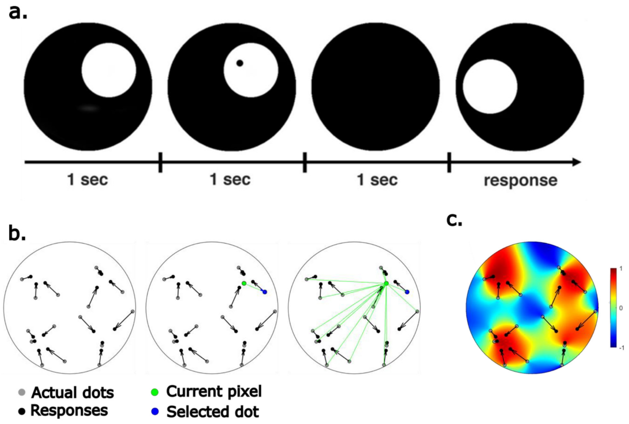

Note. (a) Example of a trial. Participants saw a gray circle appear on the screen, followed 1 s later by a small black dot (shown larger than actual size for illustrative purposes). After a 1 s delay, the white circle appeared at another location on the screen and participants used the mouse cursor to reproduce the relative location of the dot within the circle. The head of the participant was either upright or tilted 30° to the left. Participants viewed the screen through a circular aperture, which prevented the use of environmental cues. (b) Procedure to estimate the CSI maps. Error vectors for one hypothetical participant (left panel; note that in reality there were 200 dot locations, rather than 14 as in the example). A detailed description of how the CSI maps were estimated can be found in Azañón et al. (2020). In summary, we used the cosine between two vectors as a measure of similarity between their directions. One of the vectors provides information about the direction of the response error (i.e., the black arrows in the figure) that the participant made for a specific dot (e.g., the blue dot [dark grey in print version] on the right of the circle of panel b). The other vector provides information about the direction between the same specific dot (blue dot [light grey in print version]) and one pixel within the circle (e.g., the green dot) that was chosen as potential prototype location during the estimation process. This pixel represents the ending point of the predicted error vector if it was the prototype. Note that as this is a data-driven approach, all pixels within the circle are used as potential prototypes (one at a time during the iteration process). The cosine of the angle between these two vectors represents the similarity of the directions: If the cosine is 1, then the response error vector points exactly toward the selected pixel (in other words, the response is pulled toward that location); If the cosine is −1, then the response error vector points against the selected pixel (i.e., it is pushed away from that location); If the current pixel does not affect the response in any way, then the two vectors are expected to be (on average) perpendicular and the cosine is equal to 0.5. The intermediate values represent how much a predicted location affects a response (either pulling toward or repelling the responses). To estimate a CSI for a given pixel, the contribution of all cosine is taken into account (i.e., how much a specific pixel influences all responses) as illustrated in the right circle of panel b. As it is expected that a pixel influences especially neighboring responses, dots that were closer to the current pixel were given larger weights than dots further away, see the Method (Analysis) section and Azañón et al. (2020). (c) CSI map. Example of a CSI map derived from the actual dots and localization responses is shown in panel b (also reported over the CSI map). Larger reddish values indicate regions that acted as “attractors” for the responses (see how responses converge toward these regions); smaller bluish values indicate regions that “repelled” responses; Values close to zero indicate regions that did not influence the responses. CSI = cosine similarity index. See the online article for the color version of this figure.

using G*Power 3.1 software (Faul et al., 2007) using this effect size and alpha of .05 showed that our sample had a power of more than 0.95 to detect an equivalent effect. We thus believe that our sample is appropriately powered to distinguish between retinal and gravitational reference frames.

Materials and Procedure

Stimuli were shown on a 22-in. monitor with a black background (1,680 × 1,050 pixels resolution). Participants viewed the screen from a distance of 50 cm. The stimuli consisted of a black dot (0.23° of visual angle in diameter, seven pixels) which appeared inside a gray circle (RGB: 0.86, 0.86, 0.86; 16.03° of visual angle in diameter, 500 pixels). The location of the circle on the monitor varied randomly on each trial, and the dot could appear in one of 200 different locations within the circle. The distribution of dot locations was identical across participants but was different across the two conditions (tilted and straight). The configuration of the dots for each of the two conditions was reversed in half of the participants, so that the dots presented in the circle in the upright condition for half of the participants were those presented in the tilted condition for the other half, and vice versa. In creating the distribution of locations, we aimed to create a visually uniform distribution without physical overlap of the dots. The center of all dots were at least 20 pixels from the edge of the circle and the centers of pairs of dots were at least 24 pixels apart. Five additional dots were presented at the start of the experiment as practice trials, and were not analyzed. The stimuli were viewed through a shroud creating a circular aper- ture (diameter of 18.5 cm), which occluded peripheral vision and prevented participants using environmental cues such as the frame of the monitor or the alignment of walls, similar to that used in previous studies (Gallagher & Ferrè, 2018). The presentation of stimuli and collection of responses were controlled by a custom script in MATLAB (MathWorks, Natick, MA) using the Psychtoolbox (Brainard, 1997). The room was kept dark throughout the experiment.

On each trial, the circle appeared at a random location on the monitor, inside the circular space left by the cone. After one second, the dot appeared at a random location within the circle for one additional second (i.e., the encoding interval). Then the circle and dot disappeared and a blank screen was shown for one second (i.e., the retention interval). Then the circle reappeared at a different random location on the monitor and the participant’s task was to localize the relative position of the dot within the circle using the mouse. The mouse cursor appeared at the same time as the circle at a random location on the screen.

Participants placed their head on a chinrest secured to the table. In the *upright* condition, the participant positioned their head upright on the chinrest. In the *tilted* condition, the experimenter used a protractor to tilt both the chinrest and the participant’s head 30° to the left. The participant’s head was therefore fixed to the chinrest and no movements were allowed. In each condition, the participant was instructed to maintain their head position throughout each experimental block and the experimenter checked it during the block. We selected a tilt of 30° because it is a moderate tilt that can be comfortably maintained for extended periods of time, and has been used in similar perceptual studies (Beck et al., 2020).

Participants completed two blocks each of the upright and tilted conditions. The order of conditions was counterbalanced across participants using an ABBA scheme. Each block consisted of 100 trials. There was a break midway through each block (after 50 trials).

Analysis

Analysis procedures were similar to those in our recent paper (Azañón et al., 2020). For each pixel in the circle (195,200 pixels, out of the 250,000 in the 500 × 500 square in which the circle was inscribed), we calculated the "cosine similarity index" (CSI) to quantify the extent to which error vectors are attracted toward versus repelled from that location. The CSI quantifies the similarity in direction between actual error vectors and the predicted vectors if they all pointed toward that location. For each participant, we have 200 error vectors in each of the two head orientations. We excluded trials in which the response was made outside of the circle (five trials in total; 0.06%).

To obtain a CSI value for each given pixel, we calculated the cosine of the angle formed between the actual and predicted error vectors for each of the 200 error vectors. Error vectors were computed as the difference between the target dot location and the location reported from memory by the participant, while predicted vectors corresponded to the difference between the response dot and the location of the given pixel. A cosine value of 1 indicates that the direction of the error vector was identical to the predicted vector, and a value of -1 indicates that it goes in the opposite direction. Each cosine was weighted using a Gaussian window, which gave more weight to target dots close to the given pixel. The Gaussian window (w) is defined as $\boldsymbol{w(n)} = \boldsymbol{e}^{-\boldsymbol{n}^2/2\sigma^2}$ where the standard deviation corresponds to $\sigma = (\mathbf{L} - 1)/(2\boldsymbol{\alpha})$. L, as the window length, was set to 500 pixels (the diameter of the circle). α was set to 10.78 pixels as in Azañón et al. (2020) to produce a Gaussian window where the most informative range of weights, that is, from 1 to 0.1, are given to distances that are shorter than 20% of the window length L. Finally, we calculated the CSI for the pixel as a weighted mean of the individual cosines, according to the following formula:

$$\mathrm{CSI}_{xy} = \frac{\sum_{t=1}^{N} b_t \cos(\alpha_t)}{\sum_{t=1}^{N} b_t}. \tag{1}$$

This index integrates the contribution of all 200 error vectors. b_t indicates the weight given to each cosine according to the Gaussian window, and α_t indicates the angle between the actual and predicted error vectors. Note that we have implemented a toolbox to compute CSI in MATLAB using the described protocol, see https://github.com/antigosa/prototypes_toolbox.

To estimate the amount of rotation of the prototype structure in the tilted head condition, for each participant, we computed the Euclidean distance between the prototype maps in the upright and tilted head conditions. Each pixel in the maps was treated as a separate dimension and the Euclidean distance was computed using the *pdist* function in MATLAB. Only pixels inside the circle were used. We then started a procedure that rotated the tilted head prototype map up to 45° in the counterclockwise and clockwise directions with a step of 0.01°. At each iteration (i.e., tested angle), we calculated the Euclidean distance between the rotated map from the tilted condition and the unrotated map from the upright condition. The minima distance indicated the rotation angle that maximized the similarity between the prototype maps of the two conditions for that participant. The same analysis was also performed using Pearson's correlation coefficient as a measure. As the rotations that minimized the Euclidean distance were essentially identical to those that maximized the correlation ($r > .999$), only the former were reported, as the t statistics are essentially identical.

To identify pixels in the mean similarity maps that were significantly different than zero, we ran a one-sample t test across participants on CSI values at each pixel inside the circle, separately for each condition. To control for multiple comparisons, we adopted a cluster-based permutation analysis with Monte Carlo, as we previously reported (Azañón et al., 2020). This procedure is similar to methods widely used in neuroimaging to assess cluster-level significance (Maris & Oostenveld, 2007; Nichols & Holmes, 2002). In summary, we first identified clusters of pixels as neighboring pixels (i.e., that shared at least one vertex) with t values higher than $T_{\mathrm{crit}}(19) = 3.58$ ($p < .001$) and computed a cluster statistics (i.e., the sum of the individual values). Then, to build a null distribution, the same procedure was repeated 5,000 times but, at each iteration, the signs of the CSIs for randomly selected participants were flipped before computing the clusters. We finally counted the number of times the clusters individuated under the null distribution exceeded the observed clusters and the p value was computed by dividing this number by the number of iterations. Only the observed clusters that were exceeded by the permuted values less than 5% of the times ($p < .05$) were considered significant.

Transparency and Openness

We report how we determined our sample size, all data exclusions, all manipulations, and all measures in the study. The design and analysis plan for the experiments were not preregistered. Raw data and analysis scripts are available at: https://osf.io/9z54m/.

Results

Consistent with previous research (Azañón et al., 2020; Huttenlocher et al., 1991, 2004), responses in the upright head posture were biased toward the center of mass of each of the four imagery quadrants formed by bisecting the circle along the horizontal and vertical meridians (Figure 2, top panel; Figure 3). If the reference frame for this segmentation is defined with respect to gravity, the pattern of spatial prototypes should be *unchanged* in the tilted posture, since the direction of gravity is vertical and constant. Conversely, if the reference frame is determined with respect to the retina, the prototype structure should be rotated by 30°, matching the orientation of the head.

To identify the amount by which prototype structure was rotated, we calculated the Euclidean distance between the prototype maps in the upright and tilted head posture conditions. We then rotated the map in the tilted posture to identify the magnitude of rotation that minimized the Euclidean distance between the two maps (Figure 2, bottom panel). The mean angle across participants was 8.8°, significantly different from 0°, $t(19) = 6.47$, $p < .0001$, $d = 1.45$, indicating a contribution of a retinotopic frame of reference. This mean angle was also significantly different from 30°, $t(19) = 15.56$, $p < .0001$, $d = 3.48$, indicating a contribution of a gravicentric frame of reference. Finally, this mean angle was significantly smaller than 15°, $t(19) = 4.54$, $p < .001$, $d = 1.02$, indicating that the weighting given to the gravicentric reference frame was larger than that given to the retinotopic one. On average, this corresponds to a weight of 0.294 for the retinotopic frame, and 0.706 for the gravicentric one.

Figure 2

Spatial Prototypes

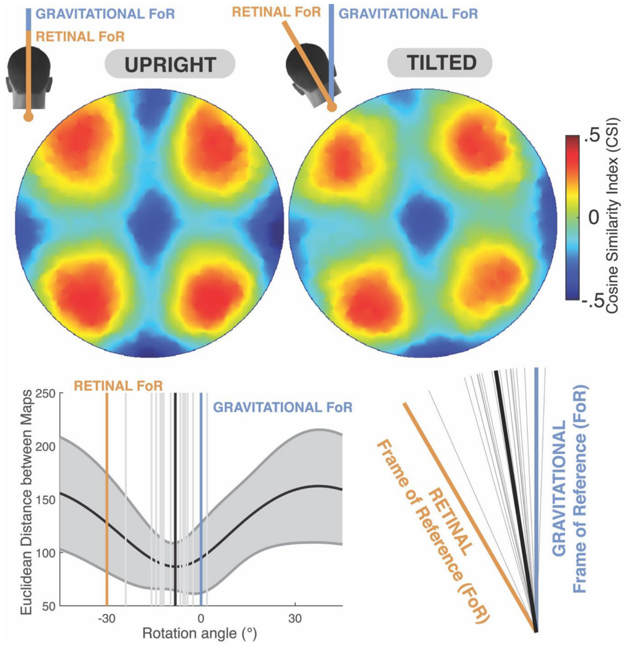

Note. Top row: By analyzing the pattern of directional memory errors, we quantified for each location in the circle whether it tended to attract or repel responses with the CSI, comparing the similarity of actual error vectors with those predicted if they were all pointing at that location. Consistent with previous work, there were four distinct spatial prototypes formed by dividing the circle along horizontal and vertical meridians. Bottom left: The Euclidean distance between prototype maps in the two head postures as a function of the degree of rotation of the map in the upright condition. The black curve shows the mean Euclidean distance between maps, and the gray-shaded region shows the 95% confidence interval. The gray vertical lines indicate the angles at which the Euclidean distance is minimized for each participant. Bottom right: Each gray line indicates the orientation of the prototype map in the upright posture for one participant. The thick black line shows the mean orientation across participants. The thick blue line indicates the orientation predicted if participants relied exclusively on a gravitational reference frame, and the thick orange line shows the orientation predicted if participants relied exclusively on a retinal reference frame. CSI = cosine similarity index; FoR = frame of reference. See the online article for the color version of this figure.

Figure 3

Statistical Parametric Maps Showing the t Statistic Calculated on CSI Values at Each Pixel Within the Circle

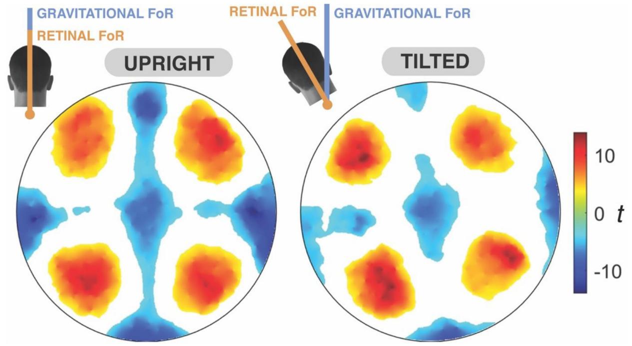

Note. Only clusters that survived correction for multiple comparison corrections are shown. CSI = cosine similarity index; FoR = frame of reference. See the online article for the color version of this figure.

Discussion

Our results show that spatial memory is determined by a dynamic combination of reference frames, with clear contributions from both gravitational and retinal factors. This is consistent with the results from our recent study (Azañón et al., 2020) in which we found that the structure of spatial prototypes was determined by a flexibly-weighted combination of reference frames determined by the intrinsic geometry of shapes (e.g., axes of symmetry) and extrinsic factors linked to the observer or the environment. The present study provides deeper insight into the nature of these extrinsic frames of reference.

In particular, we find that the weight given to gravity is substantially greater than that given to retinal orientation. There is a long-standing debate regarding the relative importance of these cues to self-orientation, with some authors emphasizing the importance of retinal (Dichgans et al., 1972; Koffka, 1935) and others gravitational (Clemens et al., 2011; Gibson & Mowrer, 1938) cues. In showing that the weighting given to gravity is greater than that given to retinal cues, our results are consistent with the interpretation of Gibson and Mowrer (1938) that gravity is "the more decisive factor in cases of real conflict between the two types of sensory data" (p. 303). It is also possible that sensory cues from other sources might influence perceived verticality, such as the so-called idiotropic vector (Merfeld et al., 1999). For example, Dyde et al. (2006) isolated independent contributions of visual, gravitational, and idiotropic reference frames to the subjective visual vertical.

Our study focused on the use of implicitly imposed horizontal and vertical meridians for spatial memory for object location but did not assess the immediate perception of stimulus orientation. Our paradigm is notably different from tasks involving explicit judgments of verticality in that participants are never instructed to judge verticality. The use of implicit vertical and horizontal axes to segment the circle in the present study is entirely automatic, and participants may even be unaware that they are dividing the shape in this way.

This simultaneous use of multiple reference frames is consistent with recent research investigating the frames of reference determining the structure of hippocampal place cells (Grieves et al., 2020) and grid cells (Casali et al., 2019) in rats, which has found a flexible integration of multiple frames of reference related to the animal's body and to gravity. While head-direction responses in rodents have generally been studied in the two-dimensional horizontal plane, studies in bats have shown that neurons in the presubiculum represent the orientation of the head in all three spatial dimensions (Finkelstein et al., 2015). While, to the best of our knowledge, no studies in humans have demonstrated similar representations, it is notable that the vestibular system provides constant sensory signals about the direction of the gravitational vector and the orientation of the head relative to gravity. We thus suggest that the vestibular system may play an important role in determining reference frames for spatial memory.

In showing that gravity is dominant over retinal cues, our results could be interpreted as evidence against the interpretation of Huttenlocher and colleagues (Engebretson & Huttenlocher, 1996;

Huttenlocher et al., 2004) that the segmentation of shapes in the formation of spatial prototypes is related to the "oblique effect" (Appelle, 1972). It is worth noting, however, that there is evidence that the orientation-selectivity of neurons in the visual system may itself be modulated by head orientation (Horn & Hill, 1969; Rosenberg & Angelaki, 2014). While the classic orientation-selectivity of the visual cortex (Hubel & Wiesel, 1998) is generally conceived as retinotopic in nature, it may be that gravity modulates even the earliest visual representations of space. It is worth noting, however, that studies have reaching inconsistent conclusions about whether such modulation is found as early as primary visual cortex (Horn & Hill, 1969) or only emerges later in the visual processing stream (Rosenberg & Angelaki, 2014).

Humans are so well adapted to the gravitational vector, that they might use it to guide behavior. For example, random accelerations are hardly perceived (Werkhoven et al., 1992), falling objects are expected to accelerate even when their velocity is constant (Zago et al., 2008), and observers generally misremember the location of moving objects in space, displacing them as if they were under the influence of terrestrial gravity (De Sá Teixeira, 2016). We can catch objects accelerating downwards with little to no effort, even when parts of the object's trajectory are occluded and no cues about position and velocity are given (Zago et al., 2005). Our results thus contribute to a growing literature showing that the gravitational vector modulates numerous aspects of perception and cognition.

One might question the exact degree of inclination of the retinotopic vertical in our experiment. Previous studies indicate that a head roll tilt induces small degree of ocular countertorsion (Howard, 1982). Accordingly, our inclination of the retinocentric vertical would have been about 26° from the gravitational vertical rather than exactly 30°. Importantly, despite the potential small discrepancy between physical versus perceived tilt, participants significantly gave more weight to the gravitational than retinal frame of reference.

Our results showing a larger role of gravity than retinotopy for spatial memory provide an interesting contrast with research on spatial memory following eye movements, which has found that memory is more precise in retinotopic than in spatiotopic coordinates (Golomb & Kanwisher, 2012; Shafer-Skelton & Golomb, 2018). This pattern makes sense given that determining spatiotopic location in this sense requires that the initial retinotopic representation in early visual cortices be "remapped" to reflect the movement of the eyes, a process that must be iteratively updated every few hundred milliseconds. Notably, however, gravity provides a stable and (except for astronauts) omnipresent reference frame, signaled by a dedicated sensory apparatus, which does not require any such process of remapping.

References

Appelle, S. (1972). Perception and discrimination as a function of stimulus orientation: The "oblique effect" in man and animals. *Psychological Bulletin*, *78*(4), 266–278. https://doi.org/10.1037/h0033117

Aubert, H. (1861). Eine scheinbare bedeutende drehung von objecten bei neigung des kopfes nach rechts oder links [An apparent significant rotation of objects when the head is tilted to the right or left]. *Archiv für pathologische Anatomie und Physiologie und für klinische Medicin*, *20*(3–4), 381–393. https://doi.org/10.1007/BF02355256

Azañón, E., Tucciarelli, R., Siromahov, M., Amoruso, E., & Longo, M. R. (2020). Mapping visual spatial prototypes: Multiple reference frames shape visual memory. *Cognition*, *198*, Article 104199. https://doi.org/10.1016/j.cognition.2020.104199

Beck, B., Saramandi, A., Ferrè, E. R., & Haggard, P. (2020). Which way is down? Visual and tactile verticality perception in expert dancers and non-experts. *Neuropsychologia*, *146*, Article 107546. https://doi.org/10.1016/j.neuropsychologia.2020.107546

Berthoz, A. (1996). How does the cerebral cortex process and utilize vestibular signals? In R. W. Baloh & G. M. Halmagyi (Eds.), *Disorders of the vestibular system* (pp. 113–125). Oxford University Press.

Brainard, D. H. (1997). The psychophysics toolbox. *Spatial Vision*, *10*(4), 433–436. https://doi.org/10.1163/156856897X00357

Bufacchi, R. J., & Iannetti, G. D. (2016). Gravitational cues modulate the shape of defensive peripersonal space. *Current Biology*, *26*(21), R1133–R1134. https://doi.org/10.1016/j.cub.2016.09.025

Campbell, F. W., Kulikowski, J. J., & Levinson, J. (1966). The effect of orientation on the visual resolution of gratings. *The Journal of Physiology*, *187*(2), 427–436. https://doi.org/10.1113/jphysiol.1966.sp008100

Casali, G., Bush, D., & Jeffery, K. (2019). Altered neural odometry in the vertical dimension. *Proceedings of the National Academy of Sciences of the United States of America*, *116*(10), 4631–4636. https://doi.org/10.1073/pnas.1811867116

Cheng, K., Shettleworth, S. J., Huttenlocher, J., & Rieser, J. J. (2007). Bayesian Integration of spatial information. *Psychological Bulletin*, *133*(4), 625–637. https://doi.org/10.1037/0033-2909.133.4.625

Clemens, I. A. H., De Vrijer, M., Selen, L. P. J., Van Gisbergen, J. A. M., & Medendorp, W. P. (2011). Multisensory processing in spatial orientation: An inverse probabilistic approach. *Journal of Neuroscience*, *31*(14), 5365–5377. https://doi.org/10.1523/JNEUROSCI.6472-10.2011

De Sá Teixeira, N. (2016). How fast do objects fall in visual memory? Uncovering the temporal and spatial features of representational gravity. *PLoS ONE*, *11*(2), Article e0148953. https://doi.org/10.1371/journal.pone.0148953

De Valois, R. L., William Yund, E., & Helper, N. (1982). The orientation and direction selectivity of cells in macaque visual cortex. *Vision Research*, *22*(5), 531–544. https://doi.org/10.1016/0042-6989(82)90112-2

Dichgans, J., Held, R., Young, L. R., & Brandt, T. (1972). Moving visual scenes influence the apparent direction of gravity. *Science*, *178*(4066), 1217–1219. https://doi.org/10.1126/science.178.4066.1217

Duffy, S., Huttenlocher, J., & Crawford, L. E. (2006). Children use categories to maximize accuracy in estimation. *Developmental Science*, *9*(6), 597–603. https://doi.org/10.1111/j.1467-7687.2006.00538.x

Dyde, R. T., Jenkin, M. R., & Harris, L. R. (2006). The subjective visual vertical and the perceptual upright. *Experimental Brain Research*, *173*(4), 612–622. https://doi.org/10.1007/s00221-006-0405-y

Engebretson, P. H., & Huttenlocher, J. (1996). Bias in spatial location due to categorization: Comment on Tversky and Schiano. *Journal of Experimental Psychology: General*, *125*(1), 96–108. https://doi.org/10.1037/0096-3445.125.1.96

Faul, F., Erdfelder, E., Land, A.-G., & Buchner, A. (2007). G*Power 3: A flexible statistical power analysis program for the social, behavioral, and biomedical sciences. *Behavior Research Methods*, *39*(2), 175–191. https://doi.org/10.3758/BF03193146

Ferrè, E. R., Frett, T., Haggard, P., & Longo, M. R. (2019). A gravitational contribution to perceived body weight. *Scientific Reports*, *9*(1), Article 11448. https://doi.org/10.1038/s41598-019-47663-x

Finkelstein, A., Derdikman, D., Rubin, A., Foerster, J. N., Las, L., & Ulanovsky, N. (2015). Three-dimensional head-direction coding in the bat brain. *Nature*, *517*(7533), 159–164. https://doi.org/10.1038/nature14031

Furmanski, C. S., & Engel, S. A. (2000). An oblique effect in human primary visual cortex. *Nature Neuroscience*, *3*(6), 535–536. https://doi.org/10.1038/75702

Gallagher, M., & Ferrè, E. R. (2018). The aesthetics of verticality: A gravitational contribution to aesthetic preference. *Quarterly Journal of*

Experimental Psychology, *71*(12), 2655–2664. https://doi.org/10.1177/1747021817751353

Gallagher, M., Kearney, B., & Ferrè, E. R. (2021). Where is my hand in space? The internal model of gravity influences proprioception. *Biology Letters*, *17*(6), Article 20210115. https://doi.org/10.1098/rsbl.2021.0115

Gibson, J. J., & Mowrer, O. H. (1938). Determinants of the perceived vertical and horizontal. *Psychological Review*, *45*(4), 300–323. https://doi.org/10.1037/h0060402

Golomb, J. D., & Kanwisher, N. (2012). Retinotopic memory is more precise than spatiotopic memory. *Proceedings of the National Academy of Sciences of the United States of America*, *109*(5), 1796–1801. https://doi.org/10.1073/pnas.1113168109

Grieves, R. M., Jedidi-Ayoub, S., Mishchanchuk, K., Liu, A., Renaudineau, S., & Jeffery, K. J. (2020). The place-cell representation of volumetric space in rats. *Nature Communications*, *11*(1), Article 789. https://doi.org/10.1038/s41467-020-14611-7

Harnad, S. (1987). *Categorical perception: The groundwork of cognition*. Cambridge University Press.

Heeley, D. W., & Timney, B. (1988). Meridional anisotropies of orientation discrimination for sine wave gratings. *Vision Research*, *28*(2), 337–344. https://doi.org/10.1016/0042-6989(88)90162-9

Horn, G., & Hill, R. M. (1969). Modifications of receptive fields of cells in the visual cortex occurring spontaneously and associated with bodily tilt. *Nature*, *221*(5176), 186–188. https://doi.org/10.1038/221186a0

Howard, I. P. (1982). *Human visual orientation*. John Wiley & Sons.

Hubel, D. H., & Wiesel, T. N. (1998). Early exploration of the visual cortex. *Neuron*, *20*(3), 401–412. https://doi.org/10.1016/S0896-6273(00)80984-8

Huttenlocher, J., Hedges, L. V., Corrigan, B., & Crawford, L. E. (2004). Spatial categories and the estimation of location. *Cognition*, *93*(2), 75–97. https://doi.org/10.1016/j.cognition.2003.10.006

Huttenlocher, J., Hedges, L. V., & Duncan, S. (1991). Categories and particulars: Prototype effects in estimating spatial location. *Psychological Review*, *98*(3), 352–376. https://doi.org/10.1037/0033-295X.98.3.352

Koffka, K. (1935). *Principles of Gestalt psychology*. Lund Humphries.

Lipinski, J., Simmering, V. R., Johnson, J. S., & Spencer, J. P. (2010). The role of experience in location estimation: Target distributions shift location memory biases. *Cognition*, *115*(1), 147–153. https://doi.org/10.1016/j.cognition.2009.12.008

Maffei, L., & Campbell, F. W. (1970). Neurophysiological localization of the vertical and horizontal visual coordinates in man. *Science*, *167*(3917), 386–387. https://doi.org/10.1126/science.167.3917.386

Mansfield, R. J. W. (1974). Neural basis of orientation perception in primate vision. *Science*, *186*(4169), 1133–1135. https://doi.org/10.1126/science.186.4169.1133

Maris, E., & Oostenveld, R. (2007). Nonparametric statistical testing of EEG- and MEG-data. *Journal of Neuroscience Methods*, *164*(1), 177–190. https://doi.org/10.1016/j.jneumeth.2007.03.024

Merfeld, D. M., Zupan, L., & Peterka, R. J. (1999). Humans use internal models to estimate gravity and linear acceleration. *Nature*, *398*(6728), 615–618. https://doi.org/10.1038/19303

Müller, G. E. (1916). Über das Aubertsche phänomen [On the Aubert phenomenon]. *Zeitschrift für Sinnesphysiologie 49*, 109–244.

Newcombe, N., & Huttenlocher, J. (2000). *Making space: The development of spatial representations and reasoning*. MIT Press.

Nichols, T. E., & Holmes, A. P. (2002). Nonparametric permutation tests for functional neuroimaging: A primer with examples. *Human Brain Mapping*, *15*(1), 1–25. https://doi.org/10.1002/hbm.1058

Orban, G. A., Vandenbussche, E., & Vogels, R. (1984). Human orientation discrimination tested with long stimuli. *Vision Research*, *24*(2), 121–128. https://doi.org/10.1016/0042-6989(84)90097-X

Rosenberg, A., & Angelaki, D. E. (2014). Gravity influences the visual representation of object tilt in parietal cortex. *The Journal of Neuroscience*, *34*(43), 14170–14180. https://doi.org/10.1523/JNEUROSCI.2030-14.2014

Shafer-Skelton, A., & Golomb, J. D. (2018). Memory for retinotopic locations is more accurate than memory for spatiotopic locations, even for visually guided reaching. *Psychonomic Bulletin & Review*, *25*(4), 1388–1398. https://doi.org/10.3758/s13423-017-1401-x

Van Beuzekom, A. D., & Van Gisbergen, J. A. (2000). Properties of the internal representation of gravity inferred from spatial-direction and body-tilt estimates. *Journal of Neurophysiology*, *84*(1), 11–27. https://doi.org/10.1152/jn.2000.84.1.11/F

Vaziri, S., & Connor, C. E. (2016). Representation of gravity-aligned scene structure in ventral pathway visual cortex. *Current Biology*, *26*(6), 766–774. https://doi.org/10.1016/j.cub.2016.01.022

Wedell, D. H., Fitting, S., & Allen, G. L. (2007). Shape effects on memory for location. *Psychonomic Bulletin & Review*, *14*(4), 681–686. https://doi.org/10.3758/BF03196821

Werkhoven, P., Snippe, H. P., & Toet, A. (1992). Visual processing of optic acceleration. *Vision Research*, *32*(12), 2313–2329. https://doi.org/10.1016/0042-6989(92)90095-Z

Zago, M., Bosco, G., Maffei, V., Iosa, M., Ivanenko, Y. P., & Lacquaniti, F. (2005). Fast adaptation of the internal model of gravity for manual interceptions: Evidence for event-dependent learning. *Journal of Neurophysiology*, *93*(2), 1055–1068. https://doi.org/10.1152/jn.00833.2004

Zago, M., McIntyre, J., Senot, P., & Lacquaniti, F. (2008). Internal models and prediction of visual gravitational motion. *Vision Research*, *48*(14), 1532–1538. https://doi.org/10.1016/j.visres.2008.04.005

Received November 1, 2022
Revision received April 5, 2023
Accepted May 4, 2023 ■